Evaluating model parameters of the κ- and β'-type Mott insulating organic solids

Takashi Koretsune[1] and Chisa Hotta[2]
[1]*Department of Physics, Tokyo Institute of Technology, Tokyo 152-8551, Japan*
[2]*Department of Physics, Kyoto Sangyo University, Kyoto 603-8555, Japan*
(Received 22 May 2013; revised manuscript received 31 October 2013; published 3 January 2014)

We elucidate the model parameters for a series of organic crystals called κ- and β'-type salts by constructing the maximally localized Wannier orbitals which reproduce the bulk energy band of the first-principles methods based on the density functional theory (DFT). These materials host a dimer Mott insulator, localizing one hole per dimerized ET molecules due to strong on-dimer interaction, $U_{\rm d}$. For all these materials, we evaluate the parameters of the two representative effective lattice models in units of molecule and on dimer, and clarify two issues. First, the conventional relationships between the two models called "dimer approximation" does not hold. Second, contrary to the previous semiempirical estimates, the degree of dimerization (which approximates $U_{\rm d}$) does not depend much on materials, and that the overall ground state properties are controlled by the degree of anisotropy of the triangular lattice, denoted as $|t_c/t_a|$ in units of dimers. We update the DFT estimates $|t_c/t_a|$ of κ-$ET_2Cu_2(CN)_3$, showing that it falls on a class of regular triangle with the strongest degree of frustration.

DOI: 10.1103/PhysRevB.89.045102 PACS number(s): 71.10.Fd, 71.15.Mb, 71.20.Rv, 75.10.Jm

Identifying the microscopic control parameter of the ground state properties such as metal-insulator transition is often an intriguing issue in strongly correlated condensed matters. One example is found in the two-dimensional organic solids based on BEDT-TTF (abbreviated as ET) molecules called κ-ET_2X, $X = Cu[N(CN)_2]Cl$ (abbreviated as κ-Cl), etc.,[1] which offers a particular class of Mott insulator with one hole localized per each dimerized two molecules.[2] This so-called dimer Mott insulator (DMI) turns into a superconducting state by the applied pressure or by the substitution of anions [$X = Cu(NCS)_2$, (i.e., κ-NCS)] referred to as "chemical pressure". Whether the pressure simply controls the bandwidth against the interaction strength or else is still unsettled. Recently, many related questions have been raised on the nature of DMI; while most of them exhibit an antiferromagnetic ordering, only κ-$ET_2Cu_2(CN)_3$ (i.e., κ-CN) is considered to form a spin liquid,[3] whose origin is not clarified. In addition, an anomalous dielectric response is observed in DMI, κ-CN,[4] and β'-ET_2ICl_2[5] (β'-ICl_2), and a multiferroic behavior is found in κ-Cl,[6] as well. Thus DMI needs to be reexamined[7,8] back to the construction of an effective model.

In theories, there are two candidates of the effective model. One is the half-filled Hubbard model in units of dimers as shown in Figs. 1(a) and 1(b), which is given as

$$\mathcal{H}_{\rm d} = \sum_{\langle\mu,\nu\rangle,\sigma} t_{\mu\nu}(\widetilde{c}^{\dagger}_{\mu\sigma}\widetilde{c}_{\nu\sigma} + {\rm H.c.}) + \sum_{\mu} U_{\rm d}\widetilde{n}_{\mu\uparrow}\widetilde{n}_{\mu\downarrow}, \quad (1)$$

where $\widetilde{c}_{\mu\sigma}$ is the annihilation operator of the orbital on a μth dimer with $\widetilde{n}_{\mu\sigma} = \widetilde{c}^{\dagger}_{\mu\sigma}\widetilde{c}_{\mu\sigma}$, $t_{\mu\nu}/V_{\mu\nu}$ are the interdimer transfer integral/Coulomb interaction, and $U_{\rm d}$ is the on-dimer Coulomb interaction. The other effective model is the 3/4-filled extended Hubbard model, which is given as

$$\mathcal{H} = \sum_{\langle i,j\rangle,\sigma} t_{ij}(c^{\dagger}_{i\sigma}c_{j\sigma} + {\rm H.c.}) + \sum_{\langle i,j\rangle} V_{ij}n_i n_j + \sum_i U n_{i\uparrow}n_{i\downarrow}. \quad (2)$$

Here $c^{\dagger}_{j\sigma}$ ($c_{j\sigma}$) is the creation (annihilation) operator of electron with spin $\sigma(=\uparrow,\downarrow)$ on jth molecular orbital, and $n_{j\sigma} = c^{\dagger}_{j\sigma}c_{j\sigma}$ and $n_j = n_{j\uparrow} + n_{j\downarrow}$ are the number operators. V_{ij}[9] and U are inter- and on-molecule interactions, respectively. The lattices in units of molecule are shown in Figs. 1(c) and 1(d). The number of energy bands is doubled from Eq. (1).

Equation (1) served as a minimal model of the κ-ET_2X for a long time.[10–13] In the early stage, the *ab initio* quantum chemistry calculations evaluated the model parameters of the isolated dimer.[14,15] However, the value of $U_{\rm d}$ is overestimated by a factor of 5 from the realistic values,[16] since the bulk screening effect is not included, and the validity of $t_{\mu\nu}$ against the bulk energy band is not examined. Recent remarkable progress is found in the first-principles density functional theories (DFT): they reproduced the bulk DFT energy bands by the tight-binding ones based on $t_{\mu\nu}$,[17–19] and developed a downfolding scheme to take in the screening effect from bands far off the Fermi level to $U_{\rm d}$.[18] Unfortunately, these studies are limited to few materials, such as κ-NCS.

Before the development of these recent first-principle schemes, the major strategy to evaluate $t_{\mu\nu}$ of Eq. (1) was to obtain the intermolecular t_{ij} in Eq. (2) by the semiempirical extended Hückel method, and to apply a so-called dimer approximation. Consider a νth dimer with two constituent molecular orbitals, $c_{i_1\sigma}$ and $c_{i_2\sigma}$, and construct the bonding and antibonding dimer orbitals written explicitly as $\widetilde{c}_{\nu\sigma} \sim (c_{i_1\sigma} \mp c_{i_2\sigma})/\sqrt{2}$. The energy difference of the two dimer orbitals amounts to $2t_1$. If t_1 is large, one may disregard the bonding orbitals off the Fermi level. The effective interdimer transfer integrals of the remaining antibonding orbitals are described as $(t_a^{\rm eff}, t_c^{\rm eff}) = ((t_3+t_4)/2, t_2/2)$ in κ and $(t_a^{\rm eff}, t_b^{\rm eff}, t_c^{\rm eff}) = (t_4/2, t_3/2, t_2 + t_5/2)$ in β'. This dimer approximation is adopted in many experiments and theories on molecular solids, while its validity was not examined. Sometimes, considering only one dimer orbital as in Eq. (1) instead of two as in Eq. (2) is also referred to as "dimer approximation". We instead call this a "single-band approximation", in order to discriminate this from the dimer approximation which we define as the treatment of constructing a single dimer orbital from the two molecular orbital as above.

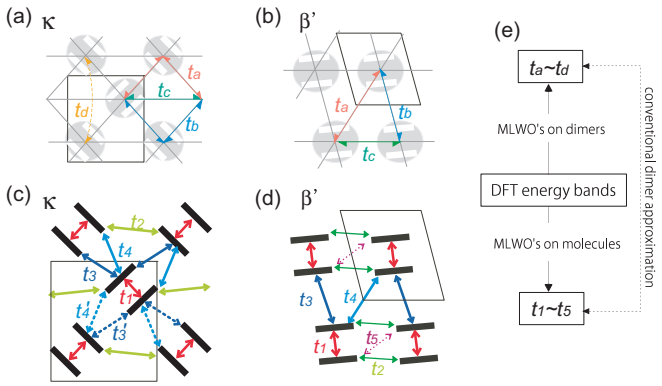

FIG. 1. (Color online) (a),(b) Simplified dimer-based anisotropic triangular lattice of κ- and β'-ET_2X. $t_{\mu\nu} = t_a \sim t_d$ are the interdimer transfer integrals in Eq. (1). (c),(d) Molecular arrangements of the two-dimensional conducting layer of κ- and β'-ET_2X. The dominant transfer integrals, $t_{ij} = t_1 \sim t_5$, of Eq. (2) are shown. (e) Scheme of DFT. The comparison of the two set of transfer integrals show that the dimer approximation does not hold.

In this paper, we perform a first systematic evaluation of the model parameters of a series of κ-ET_2X and β'-ICl_2 from first principles. We construct the maximally localized Wannier orbitals (MLWOs)[20,21] on dimer and on molecule, so as to make the corresponding tight-binding energy bands [Eq. (2) with $U = V_{ij} = 0$ and Eq. (1) with $U_d = V_{\mu\nu} = 0$] reproduce the band structures of DFT based on the experimental crystal data. (For reference, the results for the optimized structures are also shown in the Appendix.) Two main conclusions are drawn: We compare the parameters of different materials and find that on-site parameters, t_1 and U_d, are quite insensitive to the choice of materials, and that one intrinsic parameter that characterizes the DMI and the nonmagnetic/magnetic phases is "the degree of frustration" of the interdimer transfer integrals, $|t_c/t_a|$. We also examine the validity of the dimer approximation [see Fig. 1(e)]: we construct $t^{\rm eff}_{\mu\nu}$ by the linear combination of t_{ij}, compare with $t_{\mu\nu}$, and find that they do not agree, namely, the dimer approximation fails. (Note that t_{ij} and $t_{\mu\nu}$ which pick the four and two bands out of whole DFT bands are equivalent in its quality). Our results do not examine the validity of the single-band approximation, while one downfolding study on Eq. (2)[22] points out that single-band approximation may be insufficient to understand the DMI. The possible problem of adopting single-band approximation is discussed elsewhere.[7,8,23]

We perform the first-principles electronic structure calculations with the generalized-gradient approximation[25] in the framework of the DFT.[26] The ultrasoft pseudopotentials[27,28] and the plane-wave basis set with cutoff energies of 30 Ry for wave functions and 150 Ry for charge densities are used. The ground state charge densities are computed using $3 \times 4 \times 4$ and $4 \times 2 \times 4k$-point samplings for κ-CN, κ-NCS, and β'-ICl_2 and for κ-Cl and κ-Br, respectively.[29] We adopt the bare crystal data obtained by the x-ray diffraction measurements from Refs. 31,32 (κ-Cl, κ-Br, β'-ICl_2), 24, and 19 (κ-CN). In the case of κ-Cl, κ-Br, and κ-CN, we also construct the MLWOs on the anion layers as well as ET molecules for the topmost 16 valence bands including antibonding bands for κ-Cl and κ-Br and eight bands for κ-CN, since the anionic bands could not be separated from the molecular-based valence bands in these materials (see the lower bands in Fig. 2). The transfer integrals between the ET molecules and anion layers are at most 35 meV, while neglecting all of them does not change the antibonding band structures. All the transfer integrals between ET molecules other than those in Table I are less than 10 meV, and the tight-binding bands without these small contributions agree well with the DFT ones.

We first concentrate on the spin-liquid candidate, κ-CN. Figures 2(a) and 2(b) show the DFT band structures based on the crystal data by Geiser *et al.*[24] (crystal-G) and the one by Schlueter *et al.*[19] (crystal-S), respectively. In addition to the difference between the two data, the crystal structure of κ-CN has an uncertainty in the two possible orientations of the CN^- bonds in the anionic layer, which shows two different symmetries, $P2_1$ (red line) or P_c (green line). This difference does not affect the upper two bands, whereas the lower bands are extremely sensitive. However, surprisingly, the tight-binding band structures including the lower two ET bands based on $t_1 \sim t_4$ are almost identical between the two symmetries.

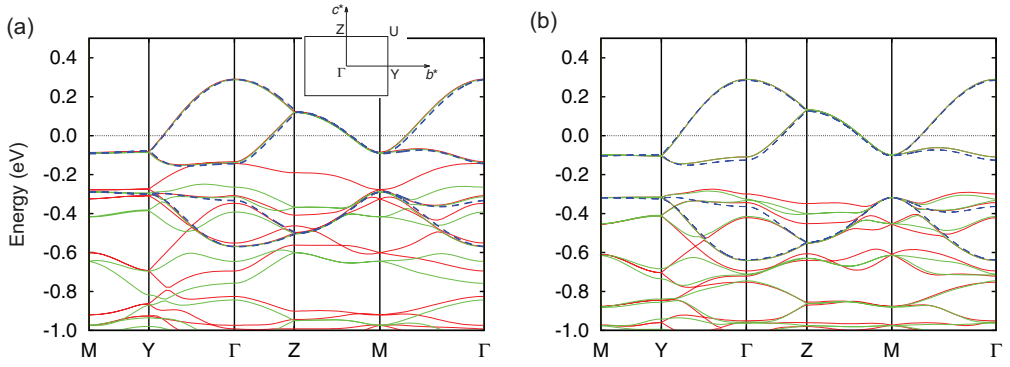

FIG. 2. (Color online) DFT band structures of κ-$ET_2Cu_2(CN)_3$ based on two different crystal data: (a) Geiser *et al.*[24] and (b) Schlueter *et al.*[19] There are two possible orientations of the CN^{-1} group with the symmetry of $P2_1$ (red lines) and P_c (green lines), respectively. However, both symmetries using t_1,t_2,t_3, and t_4 give almost the same tight-binding band structures shown in blue broken two lines put together (but are not distinguishable).

TABLE I. Tight-binding parameters of the DFT bands of a family of ET compounds given in units of meV. $t_1 \sim t_5$ are the ones based on the MLWO on a molecule (obtained via four bands), and $t_a \sim t_d$ are those of a dimer (obtained via two bands around the Fermi level in Figs. 2 and 3). (a) κ-CN is evaluated based on two different crystal data by Geiser *et al.*[24] (crystal-G) and Schlueter *et al.*[19] (crystal-S). The second column is from Ref. 18 based on crystal-G for reference. Due to symmetry lowering by the CN^{-1} group, (t_3,t_4,t_a) and (t'_3,t'_4,t_b) differ by less than 1 meV, whose averaged values are listed. (b) Several κ-type salts and β'-ET_2X materials. Crystal data are provided by Ref. 30 (κ-NCS) and Refs. 31,32 (κ-Br,Cl, β'-ICl_2). κ-d_8-Br (slowly cooled at 20 K) is at the boundary of superconducting and dimer Mott insulating phases.

(a)	Crystal-G		Crystal-S			(b) κ-NCS	d_8-Br		h_8-Cl	d_8-Cl		β'-ICl_2	
T (K)	300	Ref. 18	5	100	300	15	20	127	15	15	127	$12_{(d)}$	$_{(h)}$
t_1	180		199	196	189	200	196	195	207	209	207	251	252
t_2	82		91	88	88	72	65	63	67	68	67	−22	−24
$t_3(t'_3)$	−84		−85	−86	−78	−105 (−115)	−105	−100	−102	−102	−99	−36	−36
$t_4(t'_4)$	−24		−17	−18	−25	−39 (−15)	−39	−40	−43	−43	−42	102	100
t_5												62	62
$t_a(t_b)$	−54	−54.5 (−54.7)	−52	−52	−52	−69 (−65)	−70	−68	−70	−71	−70	49 (−26)	48 (−26)
t_c	45	44.1	51	50	47	45	38	36	37	37	36		
t_d	−7	−6.8	−7	−7	−5	−11	−10	−8	−7	−8	−8		
W	440		434	433	431	551	576	566	578	576	565	292	285
$\lvert t_c/t_a\rvert$	0.83	0.81	0.99	0.96	0.90	0.64	0.54	0.52	0.52	0.52	0.52		
$t_a^{\rm eff}$	−54		−51	−52	−52	−72 (−65)	−72	−70	−72	−72	−71	51 (−18)	50 (−18)
$t_c^{\rm eff}$	41		46	44	44	36	32	31	34	34	33	9	7
$\lvert t_c^{\rm eff}/t_a^{\rm eff}\rvert$	0.76		0.89	0.86	0.85	0.50 (0.56)	0.45	0.45	0.47	0.47	0.47		

Table I(a) shows the comparison of the tight-binding parameters evaluated by the bands with the P_c symmetry based on two different sets of crystal data. Our evaluation is in good agreement with Nakamura *et al.*[18] (P_c) based on the crystal-G and with Jeschke *et al.* ($P2_1$) based on the crystal-S. We first find that $t_1 \sim t_4$ differ significantly between the two crystal data. We also notice that constructing MLWOs of only the upper two bands, although they are seemingly in good agreement than the lower bands (see Fig. 2), also gives discrepant values of $t_a \sim t_d$. Resultantly, we find $|t_c/t_a| = 0.83$ for crystal-G and $|t_c/t_a| \sim 0.90$–0.99 for crystal-S. These values are compared with $t_a^{\rm eff}$ and $t_c^{\rm eff}$ constructed from $t_2 \sim t_4$ via dimer approximation. In all cases, the diagonal bonds, $t_a^{\rm eff}$ and t_a, agree well, whereas $t_c^{\rm eff}$ is underestimated from t_c by about 10%. Resultantly, $|t_c^{\rm eff}/t_a^{\rm eff}|$ is much smaller than $|t_c/t_a|$ obtained by the unbiased estimate. However, in the former DFT studies, these two evaluations were not properly discriminated; the two results, $|t_c/t_a| \sim |t_c/t_b| \sim 0.8$[18] (crystal-G) and $|t_c^{\rm eff}/t_a^{\rm eff}| \sim 0.8$–$0.86$[19] (crystal-S), agreed well by accident, whereas our result indicates that $|t_c/t_a| \sim 1$ (crystal-S) disagrees with the former based on crystal-G.

As a summary hereto, the value of t_c of κ-CN differs significantly between the two available crystal data. In addition, the value depends much on whether we directly obtain t_c by the upper two bands, or construct the four-band model and apply the dimer approximation to derive $t_c^{\rm eff}$. We argue that the former should be adopted instead of the latter to examine Eq. (1).

Next, we perform the same calculation on other κ- and β'-ET salts. Figure 3 shows the DFT band structures of κ- and β'-ET salts, together with the crystal structures along the conducting 2D plane where the ET molecules reside. Since the unit cell of κ-Cl/Br (h/d_8 denotes the usual/deutrated salts) is twice as large in the b (interlayer) direction compared to other κ salts, Fig. 3(b) has twice the number of bands, which have slight mixing due to the hoppings between anions and ET molecules. In the tight-binding model based on the MLWOs, these details are fully reproduced (not shown), and a single set of $t_1 \sim t_4$ gives the proper description of their mean values as shown in Fig. 3(b). In κ-NCS, the asymmetric arrangement of the anions reduces the crystal symmetry to $P2_1$ and, resultantly, t_3 and t_4 have two independent values.

Our evaluation is summarized in Table I(b). Let us compare it to the semiempirical estimates of the extended Hückel calculations in Table II. We first find one notable difference; t_1 of the Hückel data is sensitive to the choice of anions (X), which is no longer the case in our data with $t_1 \sim 200$ meV. This means that the on-dimer parameters cannot classify the difference of materials in Table I. For example, the Coulomb interaction between two electrons on an isolated dimer is represented by $U_d^{\rm iso} = 2t_1 + \frac{U}{2}\sqrt{1+(4t_1/U)^2}$ (only valid at $V_1 = 0$). Its lower bound, $2t_1$, was used as a measure of U_d[2] for convenience, since t_1 had a significant X dependence in Table II, whereas U depends not on X but only on the choice of molecule. However, this should no longer be the case. Another important feature is the inconsistency of t_2, and accordingly of $t_c^{\rm eff} = t_2/2$. In fact, our results are overall 30% smaller than the Hückel evaluation. In addition, our $t_c^{\rm eff}$ based on DFT deviates from t_c by about 10%, in the same way as κ-CN. Thus we again argue that the dimer approximation does not apply. The first report of κ-CN based on Hückel calculation and dimer approximation, $|t_c^{\rm eff}/t_a^{\rm eff}| \sim 1$, should be regarded as a "coincidence" with our DFT result without dimer approximation, $|t_c/t_a| = 0.99$ by crystal-S. At least, it is not appropriate to use $t_c^{\rm eff}/t_a^{\rm eff}$ instead of $|t_c/t_a|$ to characterize Eq. (1).

According to the experimental phase diagram on the present family of materials,[1] the system is classified from the

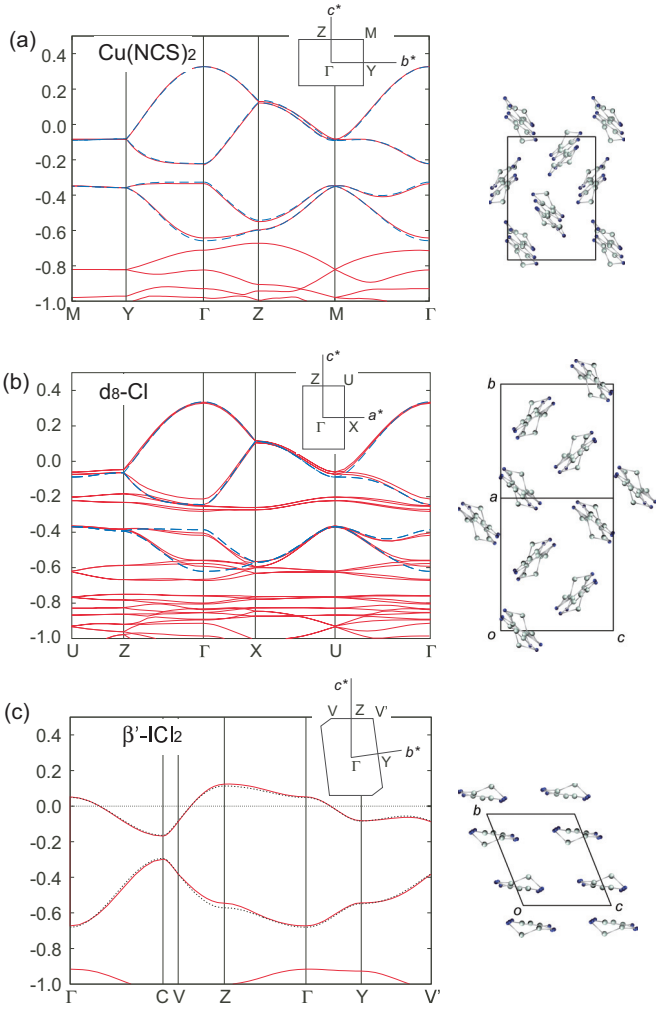

FIG. 3. (Color online) DFT band structures of (a) κ-NCS, (b) κ-d_8-Cl (deutrated), and (c) β'-ICl_2. The tight-binding band structure using $t_1 \sim t_4$ is shown together in broken lines. The crystal structures along the two-dimensional ET conducting plane are given on the right panel, where only the TTF structures of the ET molecules are shown for simplicity.

superconductor toward the DMI from left to right in Table I(b), where d-Br salt locates at the phase boundary. The experimental interpretation of the negative pressure axis along that order was the systematic variation of U_d/W, where W is the antibonding bandwidth. However, such interpretation immediately breaks down, as one sees from our first principles estimates of W. Instead, one notices that the value of t_c (or equivalently $|t_c/t_a|$) at low T could classify the superconducting NCS salt and the other three, κ-d_8-Br, h_8-Cl, and d_8-Cl, in a right order. Further, from the same geometrical point of view, the κ-CN and β'-ICl_2 differs significantly from the above four κ materials: $|t_a| \sim 50$ meV is far smaller than others. κ-CN is closer to the regular triangle. β'-ICl_2 cannot even be regarded as a triangle but an anisotropic square because $t_c \sim 0$. It should be noted that β'-ICl_2/κ-CN has far/relatively larger dimerization, $|t_1/t_a|$, than others, which is another factor to be taken into account.

To conclude, the first principles evaluation of the transfer integrals of the two representative models indicate that the overall ground state nature could be best understood by the variation of $|t_c/t_a|$, the anisotropy ratio of the triangular lattice based on dimers. Unfortunately, however, compared to other transfer integrals, the value of t_c is rather sensitive to the way it is evaluated. The dimer approximation which gives $t_c^{\rm eff}$ using molecule-based t_2 is not appropriate, and one needs to directly construct the MLWOs on dimers and evaluate t_c if one adopts Eq. (1). A proper evaluation allows the spin liquid material κ-CN to have $|t_c/t_a| \sim 1$, in contrast to the previous evaluation, $|t_c/t_a| \sim 0.85$,[18] based on different crystal data. We also point out that the degrees of dimerization of κ-CN and β'-ICl_2 differ from other DMI materials of the same organic family.

We finally anticipate on the geometry of the intersite Coulomb interaction on the basis of the crystal data. According to the down-folding studies, which evaluated the interactions by the constrained random phase approximation, the value of the screened Coulomb interaction, V_{ij}, follows $\propto 1/r$ and $\propto e^{-r/s}/r$,[37] when the three-dimensional and two-dimensional effective models are derived, respectively, where r is the distances between the center of the Wannier orbitals and s the interlayer distances. Therefore, by assuming that the Wannier center locates at the center C=C bonds of the ET molecule, one could approximately derive the values of V_{ij} within their approximation. Table III shows the results

TABLE II. Overlap integrals from the extended Hückel method in units of meV. The originally positive signs of t_3 of κ-salts are converted to negative according to the definition of Eq. (1). RT denotes the room temperature.

	κ-NCS	d_8-Br	h_8-Cl	d_8-Cl	κ-CN	β'-ICl_2	
T (K)	RT	127	15	15		RT	12
t_1	257	275.6	300.6	304.2	224	272	314
t_2	105	104.7	114.8	114.5	115	16	14
$t_3(t'_3)$	−114 (−100)	−111.5	−110.7	−109.4	−80	−16	−21
$t_4(t'_4)$	−17 (−29)	−40.4	−42.4	−42.7	−29	100	112
t_5						66	76
Ref.	36	33	33	33	34	35	32

TABLE III. Ratio of V_{ij} in unit of $V_2 = 1$, assuming that $V_{ij} \propto 1/r$ (left data) and $e^{-r/s}/r$ (right data), where r is the distances between the center C=C bonds of the ET molecules, and s the interlayer distance. The results of κ-Br, Cl, and CN salts are almost independent of the crystal data or temperature. From Ref. 18, one reads $V_2 \sim 0.4$ eV for all materials.

	κ-NCS		κ-Br/Cl/CN		β'-ICl_2	
V_1	1.78	2.15	1.8	2.2	1.12	1.19
V_3	0.96	0.95	1.2	1.3	1.30	1.47
V_4	1.00	1.01	1.0	1.0	0.57	0.39
V'_4					0.64	0.48
V_5	0.65	0.53	0.65	0.52	0.70	0.57
V_6	0.63	0.50	0.73	0.61	0.80	0.70
V_7	0.80	0.73	0.8	0.71	0.69	0.55
V_8	0.60	0.46	0.6	0.45	0.44	0.23

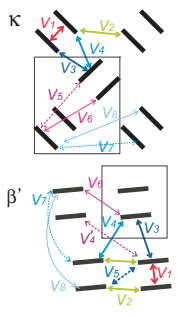

TABLE IV. Experimental and relaxed lattice parameters of κ- and β'-ET_2X materials in units of Å. Blanks for α,β, and γ indicate 90°.

	κ-CN		κ-NCS		d_8-Br		h_8-Cl		d_8-Cl		β'-ICl_2 (d)		β'-ICl_2 (h)	
	Expt.	Opt.	Expt.	Opt.	Expt.	Opt.	Expt.	Opt.	Expt.	Opt.	Expt.	Opt.	Expt.	Opt.
a	16.06	16.45	16.37	16.62	12.89	13.31	12.87	13.38	12.86	13.32	12.79	13.55	12.77	13.53
b	8.54	8.83	8.38	8.96	29.51	30.67	29.43	30.52	29.42	30.61	9.56	10.12	9.56	10.09
c	13.27	13.76	12.78	13.51	8.47	8.95	8.38	9.04	8.38	9.05	6.60	6.92	6.60	6.94
α											97.53	98.81	97.37	98.75
β	115.09	112.47	111.45	108.78							101.39	101.98	101.42	102.12
γ											86.08	90.10	86.22	90.04

based on the same crystal data with other tables. Interestingly enough, they behave nearly insensitive to the choice of anions (X). Thus one could argue that the main difference between the low temperature phases of the materials comes from the slight difference in the energy bands attributed to t_c, which is usually difficult to detect just by looking at the band structures. We also stress that a proper understanding of the low energy properties requires Eq. (2) instead of Eq. (1) as a minimal model, if we seriously take account of the effect of correlation represented by the considerably large values of V_{ij}.[22]

We thank Masashi Watanabe, Yoshio Nogami, Roser Valenti, and Harald O. Jeschke for providing us with the crystal data, and Kazuma Nakamura for discussions.

APPENDIX: TIGHT-BINDING PARAMETERS WITH STRUCTURAL OPTIMIZATION

In this appendix, we examine the effect of first-principles structural optimization on the evaluation of the model parameters. Since the organic materials are soft compared to inorganic covalent materials, predicting its optimal structures within the present scheme turns out to be quite difficult. In fact, the lattice parameters of the covalent materials after the optimization deviates from its experimental value by only about 1%, whereas we find it in the present cases to be more than 2%. Similar cases are also found in graphite, another soft material based on the van der Waals interactions, whose interlayer distance is overestimated by generalized gradient approximation. Since the transfer integrals are very sensitive to both the distances and the way of the alignment between molecules, even a seemingly small structural change by 2% significantly influences the results. This may be the reason why many preceding first principles calculations on the related organic crystals are given mostly based on the experimental crystal data without any structural optimization.

We fully relax the crystal structures and obtain the tight-binding parameters in the same way as given in the main text. For the initial structure, we choose the experimental one at the lowest temperature available. The optimization of the lattice parameters and the crystal geometries are set to have the pressures on the unit cell less than 1 kbar, and to have the force on each atom less than 0.01 eV/Å. We checked the convergence of the cutoff parameter; by taking 40 Ry for the wave functions and 200 Ry for charge densities, we find that the deviation of the lattice parameter already settles to within 0.2% to 0.3%. Table IV shows the relaxed lattice parameters. For comparison, the experimental values for the lowest-temperature structure are listed. The optimized values by DFT calculation are 2% –8% larger than the experimental ones. Due to the expansion of the unit cell most of the tight-binding parameters summarized in Table V are substantially smaller than those based on the experimental structures (see Table I in the main text for comparison). For example, the degree of dimerization, t_1, is suppressed to about 75% after the structural optimization. However, even in this quantitatively different parameter set, our main conclusions do not change; (i) the degree of dimerization does not depend much on materials (material dependence of t_1 in κ-ET_2X is less than 10 meV), and (ii) the degree of frustration, $|t_c/t_a|$, serves as the control parameter of the metal-insulator transition, properly reproducing the negative pressure effect. (iii) The $|t_c^{\rm eff}/t_a^{\rm eff}|$ which is evaluated from $t_1 \sim t_4$ by the dimer approximation does not properly reproduce the values, $|t_c/t_a|$, obtained directly from the dimer-based Wannier orbitals (single band approximation).

TABLE V. Tight-binding parameters for structure optimized κ- and β'-ET_2X materials in units of meV. These results are to be compared with Table I in the main text.

	κ-CN	κ-NCS	d_8-Br	h_8-Cl	d_8-Cl	β'-ICl_2 (d)	β'-ICl_2 (h)
t_1	146	145	154	153	151	163	166
t_2	64	42	39	33	30	−14	−15
$t_3(t'_3)$	−65	−60 (−75)	−75	−70	−72	−20	−20
$t_4(t'_4)$	−30	−32 (−17)	−31	−29	−29	84	83
t_5						31	31
$t_a(t_b)$	−48	−46	−52	−49	−49	42 (−13)	42 (−14)
t_c	35	26	24	21	19		
t_d	−4	−5	−6	−5	−6		
$\lvert t_c/t_a\rvert$	0.73	0.56	0.46	0.42	0.40		
$t_{a(b)}^{\rm eff}$	−47	−46	−53	−50	−50	42 (−10)	42 (−10)
$t_c^{\rm eff}$	32	21	19	17	15		
$\lvert t_c^{\rm eff}/t_{a(b)}^{\rm eff}\rvert$	0.68	0.45	0.37	0.34	0.30		

[1]See K. Kanoda, J. Phys. Soc. Jpn. **75**, 051007 (2006), and the references therein.
[2]See C. Hotta, Crystals **2**, 1155 (2012), and the references therein.
[3]L. Balents, Nature (London) **464**, 199 (2010).
[4]M. Abdel-Jawad, I. Terasaki, T. Sasaki, N. Yoneyama, N. Kobayashi, Y. Uesu, and C. Hotta, Phys. Rev. B **82**, 125119 (2010).
[5]S. Iguchi, S. Sasaki, N. Yoneyama, H. Taniguchi, T. Nishizaki, and T. Sasaki, Phys. Rev. B **87**, 075107 (2013).
[6]P. Lunkenheimer, J. Müller, S. Krohns, F. Schrettle, A. Loidl, B. Hartmann, R. Rommel, M. de Souza, C. Hotta, J. A. Schlueter, and M. Lang, Nat. Mater. **11**, 755 (2012).
[7]C. Hotta, Phys. Rev. B **82**, 241104 (2010).
[8]M. Naka and S. Ishihara, J. Phys. Soc. Jpn. **79**, 063707 (2010).
[9]Conventionally, the "extended Hubbard model" often refers to the one with V_{ij} between only nearest neighbor $\langle i,j\rangle$ pairs of molecular orbitals, while we also consider longer range ones.
[10]H. Morita, S. Watanabe, and M. Imada, J. Phys. Soc. Jpn. **71**, 2109 (2002).
[11]B. Kyung and A.-M. S. Tremblay, Phys. Rev. Lett. **97**, 046402 (2006).
[12]T. Koretsune, Y. Motome, and A. Furusaki, J. Phys. Soc. Jpn. **76**, 074719 (2007).
[13]R. T. Clay, H. Li, and S. Mazumdar, Phys. Rev. Lett. **101**, 166403 (2008).
[14]A. Fortunelli and A. Painelli, Phys. Rev. B **55**, 16088 (1997).
[15]E. Scriven and B. J. Powell, Phys. Rev. B **80**, 205107 (2009).
[16]F. Mila, Phys. Rev. B **52**, 4788 (1995).
[17]H. C. Kandpal, I. Opahle, Y.-Z. Zhang, H. O. Jeschke, and R. Valenti, Phys. Rev. Lett. **103**, 067004 (2009).
[18]K. Nakamura, Y. Yoshimoto, T. Kosugi, R. Arita, and M. Imada, J. Phys. Soc. Jpn. **78**, 083710 (2009).
[19]H. O. Jeschke, M. de Souza, R. Valenti, R. S. Manna, M. Lang, and J. A. Schlueter, Phys. Rev. B **85**, 035125 (2012); Information to obtain the crystal data is included. They directly fitted the four bands without constructing the MLWO, and adopted the dimer approximation to evaluate $t_a^{\rm eff} \sim t_d^{\rm eff}$.
[20]N. Marzari and D. Vanderbilt, Phys. Rev. B **56**, 12847 (1997).
[21]I. Souza, N. Marzari, and D. Vanderbilt, Phys. Rev. B **65**, 035109 (2001).
[22]K. Nakamura, Y. Yoshimoto, and M. Imada, Phys. Rev. B **86**, 205117 (2012).
[23]T. Nakano and K. Kuroki, J. Phys. Soc. Jpn. **75**, 034706 (2006).
[24]U. Geiser, H. H. Wing, K. D. Carlson, J. M. Williams, H. A. Charlier, Jr., J. E. Heindl, G. A. Yaconi, B. J. Love, M. W. Latbrop, J. E. Schirber, D. L. Overmyer, J. Ren, and M.-H. Whangbo, Inorg. Chem. **30**, 2586 (1991).
[25]J. P. Perdew, K. Burke, and M. Ernzerhof, Phys. Rev. Lett. **77**, 3865 (1996).
[26]P. Giannozzi, S. Baroni, N. Bonini, M. Calandra, R. Car, C. Cavazzoni, D. Ceresoli, G. L. Chiarotti, M. Cococcioni, I. Dabo, A. Dal Corso, S. Gironcoli, S. Fabris, G. Fratesi, R. Gebauer, U. Gerstmann, C. Gougoussis, A. Kokalj, M. Lazzeri, L. Martin-Samos, N. Marzari, F. Mauri, R. Mazzarello, S. Paolini, A. Pasquarello, L. Paulatto, C. Sbraccia, S. Scandolo, G. Sclauzero, A. P. Seitsonen, A. Smogunov, P. Umari, and R. M. Wentzcovitch, J. Phys.: Condens. Matter **21**, 395502 (2009).
[27]D. Vanderbilt, Phys. Rev. B **41**, 7892 (1990).
[28]The pseudopotentials are generated using the cutoff radii of $r_{2s} = r_{2p} = 1.1$ bohr for C and N, $r_{3s} = r_{3p} = 1.7$ bohr for S, $r_{1s} = 0.8$ bohr for H, $r_{3d} = 2.0$, $r_{4s} = 2.1$, $r_{4p} = 2.2$ bohr for Cu, $r_{3s} = r_{3p} = 1.5$ bohr for Cl, $r_{4s} = r_{4p} = 1.7$ bohr for Br, and $r_{5s} = 1.9$,$r_{5p} = 1.8$ bohr for I, respectively.
[29]We checked that calculation with cutoff energies of 40 Ry for wave functions and 200 Ry for charge densities and $4 \times 6 \times 6k$-point samplings gives almost the same results for κ-NCS and β'-ICl_2 and the difference in the tight-binding parameters is less than 1 meV.
[30]A. J. Schultz, M. A. Beno, U. Geiser, H. H. Wang, A. M. Kini, and J. M. Williams, J. Solid State Chem. **94**, 352 (1991).
[31]M. Watanabe (private communication).
[32]A. Matsunaga, Master thesis, Tohoku University, 2004.
[33]M. Watanabe, Y. Nogami, K. Oshima, H. Ito, T. Ishiguro, and G. Saito, Synth. Met. **103**, 1909 (1999).
[34]T. Komatsu, N. Matsukawa, T. Inoue, and G. Saito, J. Phys. Soc. Jpn. **65**, 1340 (1996).
[35]H. Kontani, Phys. Rev. B **67**, 180503(R) (2003).
[36]K. Oshima, T. Mori, H. Inokuchi, H. Urayama, H. Yamochi, and G. Saito, Phys. Rev. B **38**, 938 (1988).
[37]H. Shinaoka, T. Misawa, K. Nakamura, and M. Imada, J. Phys. Soc. Jpn. **81**, 034701 (2012).